JOURNAL OF GUIDANCE, CONTROL, AND DYNAMICS
Vol. 15, No. 3, May-June 1992

Dynamics of a Tethered Satellite in Elliptical, Non-Equatorial Orbits

Guido de Matteis*
University of Rome "La Sapienza," Rome, 00184 Italy

Effects of the orbit eccentricity and inclination to the equatorial plane on the stability of a tethered subsatellite are examined. For equatorial orbits, the eccentricity is seen to cause a reduction of the divergent time constant of the system in cases where the linear stability analysis predicts a parametric resonance. The orbit inclination appears to be responsible for a forced resonance phenomenon involving energy transfer from the in-plane to the out-of-plane modes.

Nomenclature

A = tether cross section
C_D = drag coefficient
E = Young's modulus
e = orbit eccentricity
i = orbit inclination
l = tether length
l_u = tether length at zero tension, reference length
m = subsatellite mass
R_0 = radius of the Keplerian orbit
R_E = Earth radius
S = subsatellite reference area
s = Laplace variable
V = relative velocity
u,v,w = velocity components
X,Y,Z = aerodynamic force components
x,y,z = subsatellite coordinates
δ = ρ/ρ_L
ϵ = stretching
θ = pitch angle
Π = gravitational constant
Π_A = $\rho_L C_D S l_u/2m$
Π_l = R_0/l_u
Π_R = R_E/l_u
Π_s = $EA/m\omega^2 l_u$
Π_ω = $1-\Omega/\omega$
Π_Ω = Ω/ω
ρ = atmospheric density
ρ_L = atmospheric density at sea level
ω = angular velocity of the reference system: ω^{-1} is the reference time
ω_e = elastic frequency
ω_l = libration frequency
Ω = Earth angular velocity

Subscript

S = steady state

I. Introduction

THIS paper is concerned with the dynamics of a tethered subsatellite system (TSS) in the presence of forcing, periodic aerodynamic actions due to the orbit eccentricity and inclination with respect to the equatorial plane. The future missions of the TSS, and in particular the TSS-2 where a subsatellite deployed as low as 120 km altitude is planned, will face the effects of an intense interaction of the system with the Earth atmosphere. When we consider that most of the TSS geophysical, atmospheric, and aerothermodynamic applications demand steady-state, constant altitude data acquisition, the importance of a complete and rigorous analysis of aerodynamic actions in the dynamic model is evident.

In previous studies, where the stability of the system following a perturbation of a stationary equilibrium was investigated,[1-4] it was shown that the aerodynamic forces can be responsible for a diverging attitude motion of the subsatellite. A possible explanation of the origin of the instability was found in a resonance phenomenon that involves aerodynamic, inertial, and elastic forces.[3] In particular, the frequency spectrum of the libration motion continously changes with the subsatellite altitude, due to the aerodynamic forces on the system, so that energy exchanges from the orbiting Shuttle to the free modes of oscillation of the TSS take place.

In this respect, a general stability criterion was determined in Ref. 3 by a linear analysis of a simple model where an elastic but massless cable and aerodynamic forces acting on the subsatellite only are considered. A more complex and complete model, accounting for the mass of the cable and for the aerodynamic forces on it, was given in Ref. 4.

In the papers just cited, the density gradient $\lambda = 1/\rho(\partial\rho/\partial x)$, where x is the vertical coordinate, was demonstrated to drive the instability phenomenon. In the practical range of subsatellite altitudes, say from 100 to 220 km, the density presents a reduction of four orders of magnitude whereas λ decreases by a factor of four only. Consequently, from a theoretical point of view, instability conditions might occur even for short, upward deployed tethers. This is a typical situation where the aerodynamic forces are, indeed, extremely small but their omission would lead to erroneous and unrealistic results in a dynamic simulation.

Once the crucial role played by aerodynamic actions has been stated in simple dynamic models, it appears obvious to bring into consideration other atmosphere related effects that were not accounted for in Refs. 3 and 4. In particular, the main objective of the present study is to develop stability criteria when the TSS moves in 1) a slightly eccentric orbit, and 2) an orbit inclined to the equatorial plane.

In fact, the eccentricity and the inclination of the orbit affect the TSS dynamics through rather different mechanisms. In the first case, we have periodic forcing aerodynamic actions in the orbital plane at the orbital frequency ω which can possibly lead to some variations in the stability criterion given in Ref. 3. This point will be discussed in Sec. II. When the orbit inclination is taken into consideration, it is well known that the rotating atmosphere drives an out-of-plane (roll) motion with frequency ω. If a linear analysis of the pertinent governing equations is carried out for a massless cable, one finds that 1) there is no coupling with the in-plane motion and

Presented as Paper 91-0532 at the 29th AIAA Aerospace Sciences Meeting, Reno, NV, Jan. 7-10, 1990; received Aug. 13, 1990; revision received June 21, 1991; accepted for publication June 25, 1991.

*Research Assistant, Department of Mechanics and Aeronautics, via Eudossiana, 18. Member AIAA.

2) the motion is always stable to small perturbations even in the presence of aerodynamic forces.[3] As a conclusion, as long as the tether is massless, the inclination should not modify the picture of a stable, slightly damped, periodic motion (the natural frequency is 2ω). It is noteworthy that the study of a massive, flexible tether in Ref. 5 predicts a growth of the roll amplitude induced by certain values of the system parameters.

It was already noted[6,7] that the periodic variation of the altitude of the subsatellite and the rotation of the atmosphere can produce aerodynamically induced resonances that are responsible for excited motions in and normal to the orbital plane.

However, if we recall some significant studies on the subject, we find that a rather wide spectrum of somehow conflicting responses results from the application of models of different complexity. In particular in Ref. 8, the important geometrical effect of the Earth oblateness on the orbital altitude was pointed out although it was neglected in the simulations, and no indication of resonance was observed. In Ref. 9, a diverging out-of-plane motion was noted and the cause of the instability found in the normal component of the atmospheric drag force: incidentally, the modeled Earth was nonspherical. In a study by Bainum et al.,[5] the divergence of the roll oscillations was related to the eccentricity of the orbit. A different interpretation of the instability mechanism was given by Kulla[10] and Spencer[11] who observed that, in inclined orbits, the oblate Earth determines density variations at a rate which is twice the orbit rate and which is resonant with the characteristic frequency of the roll motion. This concept was also reported in the review of Ref. 7 where, however, a numerical simulation which apparently included the effect of the oblate Earth showed a nearly undamped roll oscillation through an orbital period for a long cable at $i = \pi/2$.

From the cited literature, one might conclude at this point that whereas an in-plane motion presents a possible resonance instability (depending on the design parameters of the considered configuration, i.e., subsatellite mass, tether length, and orbiter altitude), the roll motion should exhibit an unstable behavior due to a forced resonance phenomenon when the orbit is inclined to the equatorial plane. A discussion of these questions will be the subject of Sec. III. One of the purposes of this paper is then to present a detailed, rigorous, and possibly complete investigation of all of the problems related with the dynamics and stability of a tethered system as influenced by aerodynamic effects.

II. Motion in Equatorial, Eccentric Orbits

Practical values of the orbit eccentricity e are extremely low in TSS applications. The effects of e on the dynamic stability of the system are thus analyzed through a power expansion of the state variables in terms of this small parameter. The solution to the pertinent equations is determined as a perturbation to the motion of a TSS with the Shuttle in a circular equatorial orbit.

Under the preceding assumptions, it is convenient to formulate the equations of motion in an orthogonal coordinate system rotating on a circular orbit with constant angular velocity[1]:

$$\omega = [\Pi(1-e^2)^3/R_0^3]^{1/2} \cong (\Pi/R_0^3)^{1/2}$$

The x axis is directed toward the Earth center and the y axis is opposite to the direction of the orbital velocity (Fig. 1).

By the use of proper reference quantities, we define the following dimensionless parameters:

$$\Pi_l = \frac{R_0}{l_u}, \qquad \Pi_s = \frac{EA}{m\omega^2 l_u}, \qquad \Pi_A = \frac{\rho_L C_D S l_u}{2m}$$

$$\Pi_\omega = 1 - \frac{\Omega}{\omega}, \qquad \delta = \frac{\rho}{\rho_L}, \qquad \Pi_R = \frac{R_E}{l_u}$$

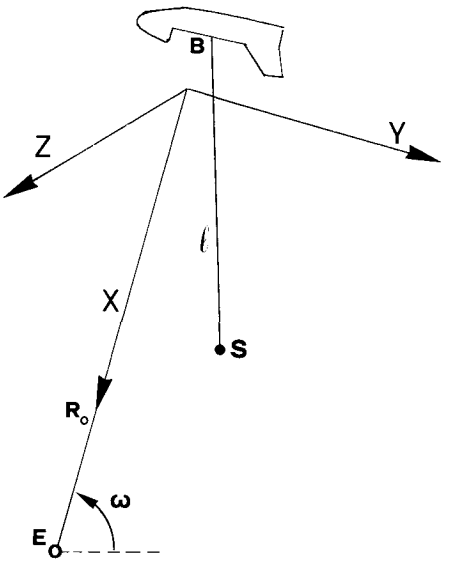

Fig. 1 Sketch of the system.

If the mass of the tether and the aerodynamic actions on it are neglected and use of the reduced gravity is made,[12] the following set of dimensionless ordinary differential equations results:

$$\dot{u} - 2v - 3x = -\Pi_s \epsilon(x - x_B)/l + X \tag{1}$$

$$\dot{v} + 2u = -\Pi_s \epsilon(y - y_B)/l + Y \tag{2}$$

$$l^2 = (x - x_B)^2 + (y - y_B)^2 \tag{3}$$

The Shuttle coordinates x_B and y_B, at the first order in e, are given by[1]

$$x_B = e\Pi_l \cos t, \qquad y_B = -2e\Pi_l \sin t \tag{4}$$

As a remark, the time is made dimensionless with respect to ω^{-1}. The Shuttle is at the perigee of its orbit at the initial time $t = 0$. The components of the aerodynamic force are

$$X = -\delta\Pi_A V u \tag{5}$$

$$Y = -\delta\Pi_A V[v - \Pi_\omega(\Pi_l - x)] \tag{6}$$

where

$$V = \{u^2 + [v - \Pi_\omega(\Pi_l - x)]^2\}^{1/2} \tag{7}$$

and

$$\delta = f(\Pi_l - \Pi_R - x) \tag{8}$$

are the velocity relative to the wind and the density, respectively.

The state vector $\xi(x,y,u,v)$ is thus expanded in powers of e, neglecting terms of order two and higher, as

$$\xi(t) = \xi_0(t) + e\xi_1(t) \tag{9}$$

The zero-order solution ξ_0 can be expressed in analytical form after Eqs. (1-8), written for $e = 0$, are linearized about a stationary equilibrium $\xi_{0_S}^T = (x_S, y_S, 0, 0)$, which can be easily determined as in Ref. 3, i.e.,

$$\xi_0(t) = \xi_{0_S} + \xi_0'(t) \tag{10}$$

and

$$\xi_0'(t) = \Phi(t)\xi_0'(0) \tag{11}$$

where $\Phi(t) = \mathcal{L}^{-1}[A^{-1}]$ is the state transition matrix, $\mathcal{L}$ indicates Laplace transform, and $\xi_0'^T(0) = (x_{0_0}', y_{0_0}', 0, 0)$. The characteristic matrix of the linear problem A is as follows:

$$A = \begin{bmatrix} s & 0 & -1 & 0 \\ 0 & s & 0 & -1 \\ \Pi_s \frac{x_S^2}{l_S^3} & \Pi_s \frac{x_S y_S}{l_S^3} & s - X_u & -2 \\ \Pi_s \frac{x_S y_S}{l_S^3} - Y_x & \Pi_s \left(\frac{y_S^2}{l_S^3} + \frac{\epsilon_S}{l_S} \right) & 2 & s - Y_v \end{bmatrix} \tag{12}$$

where s is the Laplace variable and the aerodynamic derivatives are

$$X_u = -\delta_S \Pi_A \Pi_\omega (\Pi_l - x_S) \tag{13a}$$

$$Y_v = -2\delta_S \Pi_A \Pi_\omega (\Pi_l - x_S) \tag{13b}$$

$$Y_x = \delta_S \Pi_A \Pi_\omega^2 (\Pi_l - x_S) \left[-2 + \frac{1}{\delta_S} \frac{\partial \delta}{\partial x}\bigg|_S (\Pi_l - x_S) \right] \tag{13c}$$

The first-order analysis is based on the following nonhomogeneous equation with time-varying coefficients

$$\dot{\xi}_1 = B(t)\xi_1 + C(t)\eta \tag{14}$$

with initial conditions

$$\xi_1(0) = (\Pi_l, 0, 0, -2\Pi_l)$$

where

$$\eta^T = (\Pi_l \cos t, \; -2\Pi_l \sin t)$$

and the matrices B and C depend on the system parameters and on $\xi_0^T(t) = (x_0, y_0, u_0, v_0)$, namely,

$$B = \begin{bmatrix} 0 & 0 & 1 & 0 \\ 0 & 0 & 0 & 1 \\ 3 - \Pi_s \left[1 - \frac{1}{l_0} \left(1 - \frac{x_0^2}{l_0^2} \right) \right] & -\Pi_s \frac{x_0 y_0}{l_0^3} & -\delta_0 \Pi_A V_0 \left(1 + \frac{u_0^2}{V_0^2} \right) & 2 - \delta_0 \Pi_A \frac{u_0}{V_0} \gamma \\ -\delta_0 \Pi_A \frac{u_0}{V_0} \left(\gamma \beta_\omega + \frac{1}{\delta_0} \frac{\partial \delta_0}{\partial x_0} \right) & & & \\ -\Pi_s \frac{x_0 y_0}{l_0^3} - \delta_0 \Pi_A V_0 & -\Pi_s \left[1 - \frac{1}{l_0} \left(1 - \frac{y_0^2}{l_0^2} \right) \right] & -2 - \delta_0 \Pi_A \frac{u_0}{V_0} \gamma & -\delta_0 \Pi_A V_0 \left(1 + \frac{\gamma^2}{V_0^2} \right) \\ \times \left(1 - \frac{\gamma^2}{V_0^2} \beta_\omega + \frac{1}{\delta_0} \frac{\partial \delta_0}{\partial x_0} \right) & & & \end{bmatrix} \tag{15}$$

$$C = \begin{bmatrix} \Pi_s \left[1 - \frac{1}{l_0} \left(1 - \frac{x_0^2}{l_0^2} \right) \right] & \Pi_s \frac{x_0 y_0}{l_0^3} \\ \Pi_s \frac{x_0 y_0}{l_0^3} & \Pi_s \left[1 - \frac{1}{l_0} \left(1 - \frac{y_0^2}{l_0^2} \right) \right] \end{bmatrix} \tag{16}$$

with $\gamma = v_0 - \pi_\omega(\Pi_l - x_0)$.

The solution to Eq. (14), where $\xi_0(t)$ is given by Eq. (10), is obtained by using a standard, fourth-order, rational Runge-Kutta method. As for the atmospheric density, with reference to Eq. (8), in all of the calculations the tabulated values reported in Ref. 13 were interpolated. In what follows the value of certain parameters is kept constant, as indicative of practical design conditions. In particular, we take $EA = 2 \times 10^4$ N, $R_0 = 6.5779 \times 10^6$ m, $\Omega = 7.3 \times 10^{-5}$ s^{-1}, and $C_D S = 2$ m^2. The first calculations are relative to a configuration having $m = 500$ kg and $l_u = 60$ km. In this case, when $e = 0$, the periodic motion of the subsatellite is stable although nearly undamped. The eigenvalues of A are $\sigma_{1,2} = -4.7 \times 10^{-5} \pm 1.74i$ and $\sigma_{3,4} = -7 \times 10^{-5} \pm 21.7i$, which correspond to the libration and elastic mode, respectively.

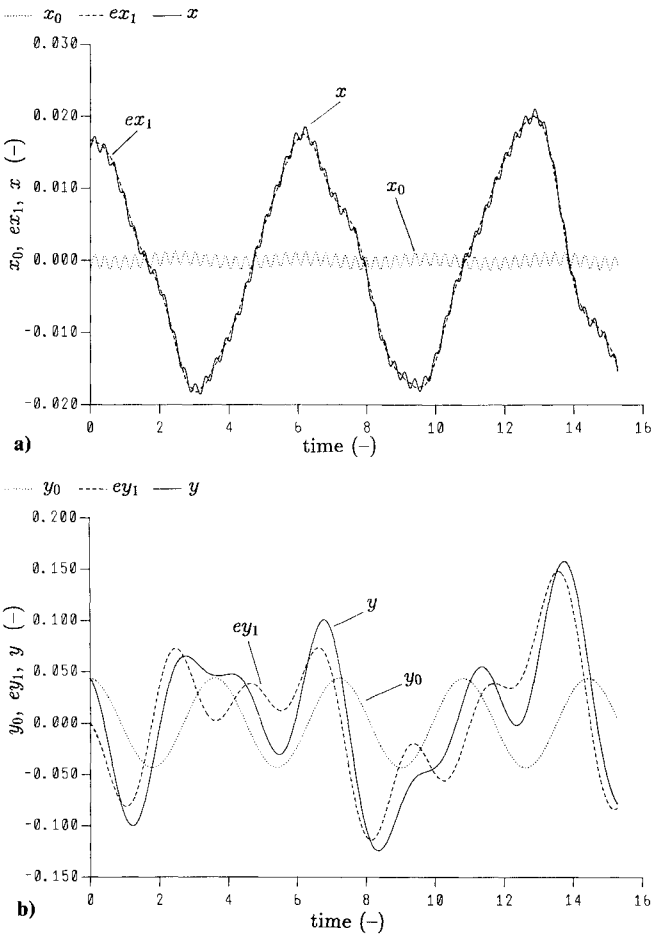

Fig. 2 Time history of a) the vertical x and b) the horizontal y displacements relative to the initial state: $l_u = 60$ km, $m = 500$ kg, $e = 1.5 \times 10^{-4}$.

Figures 2a and 2b report the time histories of the subsatellite vertical and horizontal displacements relative to the stationary equilibrium (x_S, y_S), and their components x_0, ex_1 and y_0, ey_1, respectively. With reference to Eqs. (10) and (11), the perturbation of the equilibrium state is $x_{0_0}' = \kappa x_{0_S}$, $y_{0_0}' = [l_S^2 - (x_0'(0))^2]^{1/2}$ where $\kappa = 1 \times 10^{-3}$. The very small value of the eccentricity is $e = 1.5 \times 10^{-4}$ leading to a 2-km maximum variation of the Shuttle altitude. From the figure, there is no

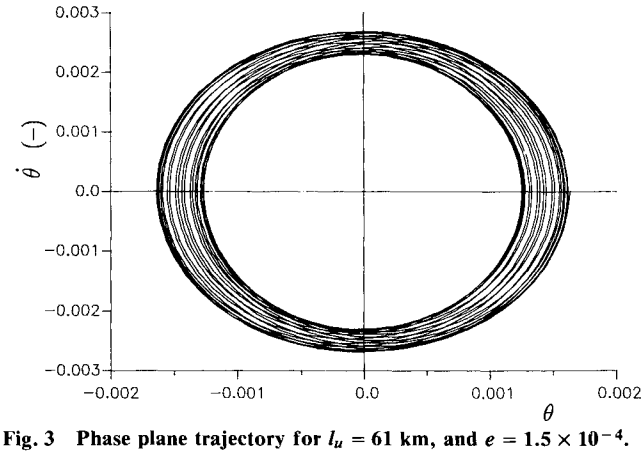

Fig. 3 Phase plane trajectory for $l_u = 61$ km, and $e = 1.5 \times 10^{-4}$.

evidence of a divergent motion which might result from the forcing action. More important, the disturbed motion displays an irregularly oscillating behavior which, as we will see, has implication in the stability analysis. For the sake of clarity, in the sequel we will consider the behavior of the pitch angle θ and of the pitch rate $\dot{\theta}$. When the frequency spectrum of $\theta - \theta(0)$ is calculated, one finds the three peaks corresponding to the libration and elastic frequencies, i.e., $\omega_l = 2.1 \times 10^{-3}$ s^{-1} and $\omega_e = 2.6 \times 10^{-2}$ s^{-1}, respectively, and to the frequency $\omega = 1.2 \times 10^{-3}$ s^{-1} of the forcing aerodynamic actions.

As for the stability analysis of Eq. (12), the nonconservative character of the dynamical system, when the aerodynamic forces are included in the model, prevents us from applying conventional energy methods or from constructing a Lyapunov function. Similarly, due to the kind of aperiodic libration motion depicted in Fig. 2a, it is not possible to formulate a dynamic stability requirement by evaluating, for instance, the variation of a positive definite function, i.e., the kinetic energy, over a few periods. Consequently, a parametric analysis is carried out, and the phase plane trajectories of the solution are obtained in a number of significant situations. The objective is, at this point, to consider limit values, in term of stability, of the system parameters and to determine if, due to the orbit eccentricity, a divergent dynamic behavior appears.

In this respect, Fig. 3 reports the phase plane trajectory in a situation such that, for $e = 0$, the linear analysis in Ref. 3 predicts limit stability conditions, namely $\mathfrak{R} = 0$, where $\mathfrak{R}$ is the Routh's discriminant of the matrix A. The final time for the simulations is $t = 70$ corresponding to 11 orbits of the main satellite. The solution for $e = 0$ is an ellipse with semiminor and semimajor axes given by $\theta = 1.6 \times 10^{-3}$ and $\dot{\theta} = 2.8 \times 10^{-3}$, respectively. The figure shows that, when $e = 1.5 \times 10^{-4}$, the trajectory is bounded by two limit cycles, whose relative distance depends on the value of e. The same nondivergent behavior is apparent for e as high as 1.5×10^{-3}, which causes an altitude variation of 20 km of the system.

The solution shown in Fig. 4 is relative to a set of parameters representative of the TSS-2 mission, i.e., $l_u = 100$ km and a Shuttle altitude of 200 km. In this case, the linear analysis indicates an unstable motion ($\mathfrak{R} = -2.7 \times 10^{-3}$), which is confirmed in Fig. 4a, obtained for $e = 0$. The effect of a small eccentricity $e = 1.5 \times 10^{-4}$ is reported in Fig. 4b. The maximum value of the pitch angle and, consequently, of the subsatellite displacement is several times larger than for $e = 0$. The trajectory center shifts alternately from one side of the phase plane to the other. As a remark on the very crucial role played by the Earth atmosphere in the case of long tethers, the elliptic trajectory corresponding to the same value of e as that just given has $\theta = 9.8 \times 10^{-4}$ and $\dot{\theta} = 1.7 \times 10^{-3}$ as semiaxes when the aerodynamic forces on the subsatellite are neglected.

Figure 5 illustrates the effect of $e = 1.5 \times 10^{-4}$ on the maximum horizontal displacement of the subsatellite, relative to the Shuttle, namely, $\Delta y_e = y(t) - y(0) - y_B(t)$, calculated over a time interval of 11 orbits. The ratio $\Delta y_e / \Delta y$, where Δy is evaluated for $e = 0$, is reported as a function of the tether length for subsatellite masses of 500 and 1000 kg. An initial perturbation of y equal to $100/l_u$ was given in all of the calculations. In the considered cases, the eccentricity has, practically, no influence on the oscillations for tethers shorter than 80 km whereas, for longer cables, we see that the subsatellite experiences much greater oscillations than for a circular orbit. The figure also shows that the relative displacement decreases for heavier subsatellites (the relative contribution of the aerodynamic forcing action is smaller) even though, from the point of view of stability, a larger mass leads to an increased rate of divergence (the elastic energy of the system, responsible of the instability, is increased). As an example, for $l_u = 100$ km, the negative damping is $\zeta = -1.1 \times 10^{-2}$ and -1.9×10^{-2} for $m = 500$ and 1000 kg, respectively.

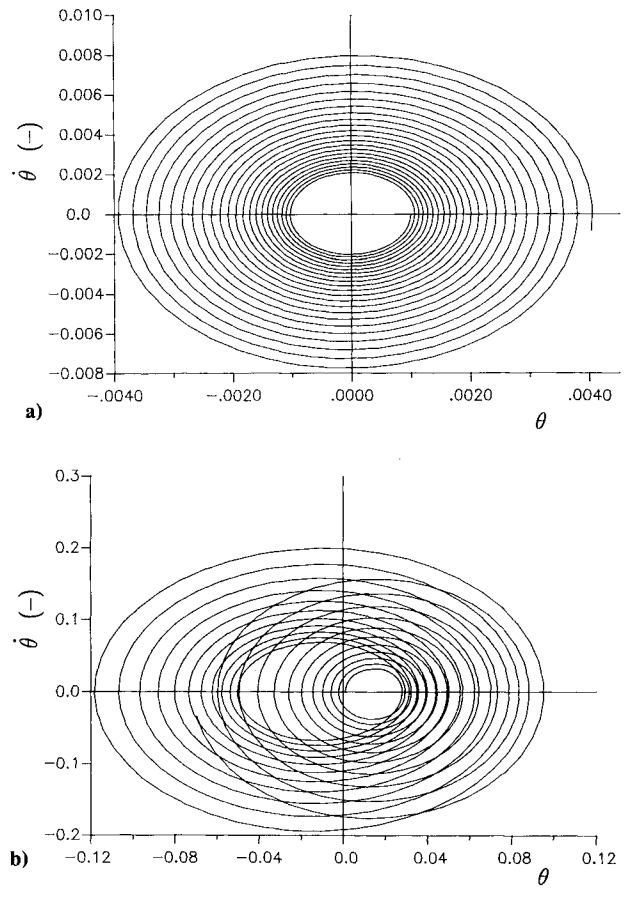

Fig. 4 Phase plane trajectories for $l_u = 100$ km: a) $e = 0$, and b) $e = 1.5 \times 10^{-4}$.

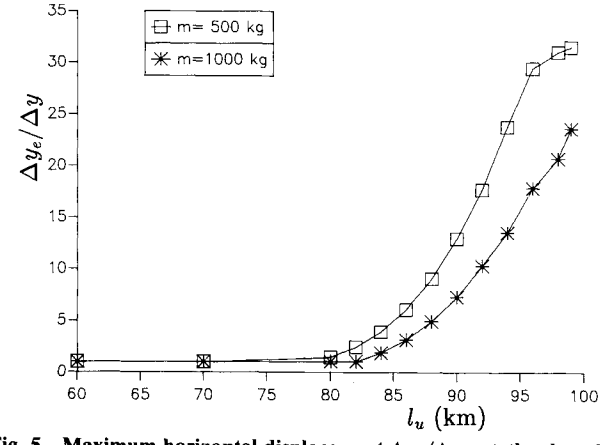

Fig. 5 Maximum horizontal displacement $\Delta y_e / \Delta y$ vs tether length l_u and subsatellite mass m.

III. Motion in Inclined Orbits

In the next part of the paper, the TSS motion in a orbit inclined with respect to the equatorial plane is discussed. The forcing action is, again, due to a variable aerodynamic force and it is now twofold. First, the rotation of the atmosphere determines the insurgence of a periodic roll motion. Second, the Earth oblateness causes a variation of the effective altitude of the subsatellite at twice the orbit rate. For a polar orbit the maximum altitude variation is as high as 20 km, corresponding to an eccentricity of 1.5×10^{-3} when reference is made to the results shown in the previous section.

Under the same hypotheses outlined in the first part of the paper, neglecting the dynamical effect due to a nonspherical gravitational field,[8] and for $e = 0$, the three-dimensional governing equations are as follows:

$$\dot{u} - 2v - 3x = -\Pi_s \epsilon x/l + X \tag{17}$$

$$\dot{v} + 2u = -\Pi_s \epsilon y/l + Y \tag{18}$$

$$\dot{w} + z = -\Pi_s \epsilon z/l + Z \tag{19}$$

$$l^2 = x^2 + y^2 + z^2 \tag{20}$$

As for the aerodynamic force components, after some small terms have been neglected, X is given by Eq. (5), and Y and Z are

$$Y = -\delta \Pi_A V[v - (\Pi_l - x)(1 - \Pi_\Omega \cos i)] \tag{21}$$

$$Z = -\delta \Pi_A V[w + (\Pi_l - x)\Pi_\Omega \sin i \cos t] \tag{22}$$

where i is the orbit inclination, and the relative wind velocity V is

$$V = \{u^2 + [v - (\Pi_l - x)(1 - \Pi_\Omega \cos i)]^2 + [w + (\Pi_l - x)\Pi_\Omega \sin i \cos t]^2\}^{1/2} \tag{23}$$

The density is

$$\delta = f[\Pi_l - \Pi_R(i,t) - x] \tag{24}$$

where $\Pi_R(i,t)$ is the dimensionless local radius of the Earth ellipsoid and it is $t = 0$ in the ascending node of the orbit.

Let us discuss the mechanism of possible out-of-plane instability. To this end, the first step is to solve numerically Eq. (19), by the same method used in Sec. II, for $l_u = 60$ km, $m = 500$ kg, and $i = \pi/2$, setting x and y constantly equal to their equilibrium values. The resulting time history of z shows no indication of a resonance instability. In fact, assuming that

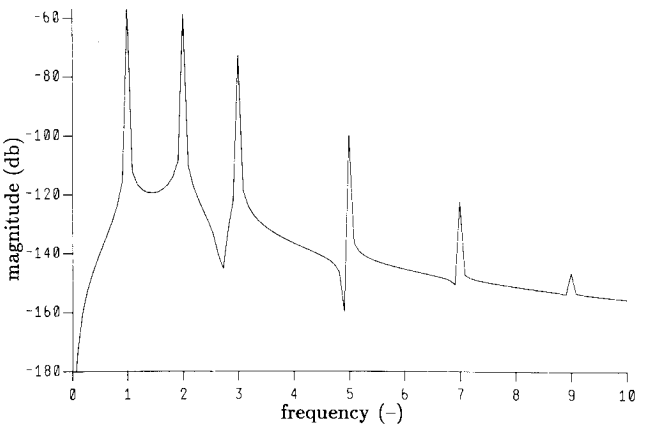

Fig. 6 Fast Fourier transform of $z - z(0)$: $i = \pi/2$, $l_u = 60$ km, $m = 500$ kg, $y = y_S$, and $x = x_S$.

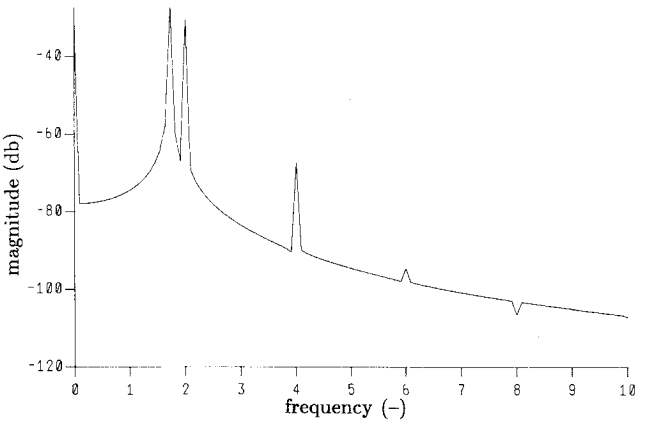

Fig. 7 Fast Fourier transform of $y - y(0)$ $i = \pi/2$, $l_u = 60$ km, and $m = 500$ kg.

the time dependence of the density, due to the oblate Earth, can be represented by a Fourier series as follows:

$$\delta = \delta_0 + \delta_1 \cos 2t + \delta_2 \cos 4t + \cdots \tag{25}$$

and substituting in Eq. (22), where V is calculated for $u = v = 0$, we find, after neglecting small terms, that the forcing term is

$$Z \cong -\Pi_A(\Pi_l - x_S)^2 \cos t(\delta_0 + \delta_1 \cos 2t + \delta_2 \cos 4t + \cdots)$$

which leads to the dimensionless frequencies of 1, 3, 5, and higher harmonics for the aerodynamic forcing action. This can also be observed in Fig. 6 where the frequency spectrum of the out-of-plane displacement z is reported. The three larger amplitudes are associated with frequency values of 1, 2 (the natural frequency), and 3.

When the full set of governing equations [Eqs. (17-20)] is solved, we note the following: 1) the three-dimensional perturbed motion is limited; 2) the in-plane and out-of-plane oscillations are uncoupled, which is correct in view of the small perturbations involved; and 3) the in-plane forcing frequency is 2 since, from Eqs. (21) and (23), we see that the largest term in the Y force expression is $-\delta \Pi_A \Pi_l^2$ where δ is given by Eq. (25). Figure 7 shows the spectrum of the computed y displacement. The two peaks on the left are at $\sqrt{3}$ (the libration frequency) and 2.

Consider now the case of a long tether, i.e., $l_u = 90$ km. The pertinent result is illustrated in Fig. 8. Both the pitch and roll motions present a divergent behavior. Because of the large amplitude of the in-plane oscillations, we note a one-way coupling in the sense that the out-of-plane solution is affected by the in-plane motion but not vice versa. Although there is no in-plane resonance (the y displacement is of comparable magnitude to the one which is observable for an eccentricity leading to the same maximum altitude variation), there is evidence that a resonance phenomenon takes place, which involves the forced libration mode at the excitation frequency 2 and the roll mode at the same value.

As a consequence of this rather complex mechanism connected with the out-of-plane stability, we see that, for a buildup of the roll oscillations, it is necessary to realize the combined effects of both a large displacement in pitch, namely, a subsatellite deployment at low altitude, and an inclined orbit. Therefore, Fig. 9 reports the effects of the tether length and of the orbit inclination on the maximum value of the out-of-plane displacement (Δz) over a time period of six orbits. We see that Δz is rather small for l lower than 80 km, whereas, for longer cables, it shows an exponential increase. For a small value of i ($i = \pi/6$) and for cables shorter than 95 km, the amplitude of the roll oscillations is only slightly reduced as compared to the results at $i = \pi/2$. In this

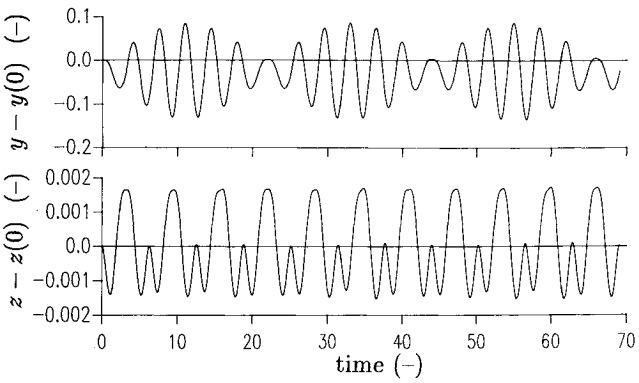

Fig. 8 Time histories of the $y-y(0)$ and $z-z(0)$ displacements: $i=\pi/2$, $l_u=90$ km, and $m=500$ kg.

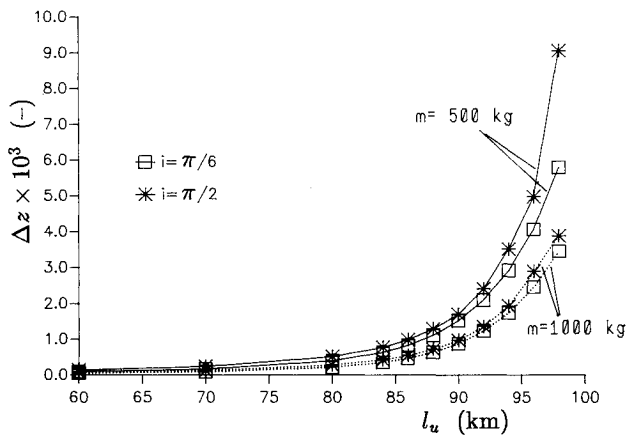

Fig. 9 Maximum out-of-plane dimensionless displacement Δz vs tether length l_u, subsatellite mass m and orbit inclination i.

respect, we have to note the two conflicting effects of i, namely, the excitation of the lateral motion due to the rotation of the atmosphere, whose magnitude increases with i, and the variation of the local altitude above the Earth surface. The latter is such that, as the inclination increases, the mean altitude of the subsatellite increases so that the aerodynamic actions turn out to be weaker. The figure also shows that the effect of the subsatellite mass on Δz is similar to the one discussed in the analysis of the libration motion in the presence of an orbit eccentricity (Fig. 5).

IV. Conclusions

In this study, the effects of the orbit eccentricity and of the inclination to the equatorial plane on the stability of a tethered subsatellite system have been discussed. In the first circumstance, a series expansion provides a perturbation solution for small e. A parametric investigation shows that the stability criterion established for the motion in a circular orbit still holds and that the eccentricity determines a sharp reduction of the divergent time constant of the system which is experienced for $e=0$.

In the inclined case, the numerical results confirm the occurrence of a aerodynamically induced resonance and allow for a complete explanation of the phenomenon, where energy is pumped from the in-plane to the out-of-plane modes leading to a buildup of the roll oscillations. This mechanism, which was apparently misinterpreted in previous studies, involves a one-way coupling of the in and normal to the orbit motions and is, in our opinion, relevant as far as the control and stabilization of the system is concerned. In fact, where long tethers are considered for applications and whenever it is required to keep the lateral displacement of the subsatellite within assigned limits rather than to bring it to zero, it can be sufficient to damp the libration motion to a point where the coupling is avoided.

At this point, it appears appropriate to refer to a reviewer's comment about a future interesting issue concerning the behavior of the system if the mass and lateral vibrations of the tether are considered. A few calculations were carried out and the results showed that, at least qualitatively, for cables of 60 km and longer, there are not appreciable differences in comparison with what has been discussed.

As a final conclusion, we would stress the fact that the Earth atmosphere, in low altitude stationkeeping, appears to affect the dynamic response of the system to an extent which has to be taken into proper consideration.

References

[1]Beletskii, V. V., and Levin, E. M., "Dynamics of the Orbital Cable Systems," *Acta Astronautica,* Vol. 12, May 1985, pp. 285–291.

[2]Onoda, J., and Watanabe, N., "Tethered Subsatellite Swinging from Atmosphere Gradients," *Journal of Guidance, Control, and Dynamics,* Vol. 11, Sept.-Oct. 1988, pp. 477–479.

[3]de Matteis, G., and de Socio, L. M., "Equilibrium of a Tether-Subsatellite System," *European Journal of Mechanics, Pt. A/Solids,* Vol. 9, May 1990, pp. 207-224.

[4]de Matteis, G., and de Socio, L. M., "Dynamics of a Tethered Satellite Subjected to Aerodynamic Forces," *Journal of Guidance, Control and Dynamics*, Vol. 14, No. 6, 1991, pp. 1129–1135.

[5]Bainum, P. M., Diarra, C. M., and Kumar, V. K., "Shuttle-Tethered Subsatellite System Stability with a Flexible Massive Tether," *Journal of Guidance, Control, and Dynamics,* Vol. 8, March–April 1985, pp. 230–234.

[6]Baker, W. P., et al., "Tether Subsatellite Study," NASA TMX-73314, March 1976.

[7]Bainum, P. M., and Kumar, V. K., "Optimal Control of the Shuttle Tethered Subsatellite System," *Acta Astronautica,* Vol. 7, Nov.-Dec. 1980, pp. 1333–1348.

[8]Misra, A. K., and Modi, V. J., "A Survey on the Dynamics and Control of Tethered Satellite Systems," *Advances in Astronautical Sciences,* Vol. 62, 1987, pp. 667–719.

[9]Kalaghan P. M., et al., "Study of the Dynamics of a Tethered Satellite System (Skyhook)," Final Rept., Contract NAS8-32199, March 1978.

[10]Kulla, P., "Stabilization of Tethered Satellites," European Space Agency, Rept. TMM/78-07/PK/avs., Dec. 1977.

[11]Spencer, T. M., "Atmospheric Perturbations and Control of a Shuttle Tethered Satellite," Paper 79-165 of the 8th IFAC Space Symposium, Oxford, U. K., July 1979.

[12]Arnold, D. A., "Tether Tutorial," *Proceedings of the Conference on Space Tethers for Science in the Space Station Era,* edited by L. Guerriero, and I. Bekey, Societa' Haliana di Fisica, Bologna, Italy, 1988, pp. 26–36.

[13]U.S. Standard Atmosphere, N.O.A.A., N.A.S.A., U.S.A.F., Washington, DC, 1976.